

- [1] S. Iijima, *Nature* **1991**, 56, 354. b) Y. Feldman, E. Wasserman, D. J. Srolovitz, R. Tenne, *Science* **1995**, 267, 222.
- [2] a) J. Hu, T. W. Odom, C. M. Lieber, *Acc. Chem. Res.* **1999**, 32, 435. b) X. Duan, C. M. Lieber, *Adv. Mater.* **2000**, 12, 298.
- [3] a) H. Dai, E. W. Wang, Y. Z. Lu, S. S. Fan, C. M. Lieber, *Nature* **1995**, 374, 769. b) Y. Li, G. W. Meng, L. D. Zhang, F. Philipp, *Appl. Phys. Lett.* **2000**, 76, 2011.
- [4] Y. C. Choi, W. S. Kim, Y. S. Park, S. M. Lee, D. J. Bae, Y. H. Lee, G. S. Park, W. B. Choi, N. S. Lee, J. M. Kim, *Adv. Mater.* **2000**, 12, 746.
- [5] a) C. C. Chen, C. C. Yeh, *Adv. Mater.* **2000**, 12, 738. b) Y. Wu, P. Yang, *Chem. Mater.* **2000**, 12, 605.
- [6] T. J. Trentler, K. M. Hickman, S. C. Goel, A. M. Viano, P. C. Gibbons, W. E. Buhro, *Science* **1995**, 270, 1791.
- [7] P. Yang, C. M. Lieber, *Science* **1996**, 273, 1836.
- [8] Y. Q. Zhu, W. B. Hu, W. K. Hsu, M. Terrones, N. Grobert, J. P. Hare, H. W. Kroto, D. R. M. Walton, H. Terrones, *J. Mater. Chem.* **1999**, 9, 3173. b) Z. L. Wang, R. P. Gao, J. L. Gole, J. D. Stout, *Adv. Mater.* **2000**, 12, 1938.
- [9] Z. G. Bai, D. P. Yu, H. Z. Zhang, Y. Ding, X. Z. Gai, Q. L. Hang, G. C. Xiong, S. Q. Feng, *Chem. Phys. Lett.* **1999**, 303, 311.
- [10] M. H. Huang, Y. Wu, H. Feick, N. Tran, E. Weber, P. Yang, *Adv. Mater.* **2001**, 13, 113.
- [11] a) C. G. Granqvist, *Appl. Phys. A: Solids Surf.* **1993**, 57, 19. b) I. Hamburg, C. G. Granqvist, *J. Appl. Phys.* **1986**, 60, R123.
- [12] a) H. J. Zhou, W. P. Cai, L. D. Zhang, *Appl. Phys. Lett.* **1999**, 75, 495. b) M. S. Lee, W. C. Choi, E. K. Kim, C. K. Kim, S. D. K. Min, *Thin Solid Films* **1996**, 279, 1.
- [13] H. Yumoto, T. Sako, Y. Gotoh, K. Nishiyama, T. Kaneko, *J. Cryst. Growth* **1999**, 203, 136.
- [14] Z. W. Pan, Z. R. Dai, Z. L. Wang, *Science* **2001**, 291, 1947.
- [15] a) X. F. Duan, C. M. Lieber, *J. Am. Chem. Soc.* **2000**, 122, 188. b) W. Han, S. Fan, Q. Li, Y. Hu, *Science* **1997**, 277, 1287.
- [16] M. Yazawa, M. Koguchi, A. Muto, K. Hiruma, *Adv. Mater.* **1993**, 5, 577.
- [17] *Smithells Metals Reference Book*, 6th ed. (Ed: E. A. Brandes), Butterworths, London **1983**, pp. 12–18.
- [18] Y. Ohhata, F. Shinoki, S. Yoshida, *Thin Solid Films* **1979**, 59, 255.
- [19] For In_2O_3 , $m_e = 0.3 m_0$, $m_h = 0.6 m_0$, $\epsilon = 9$ [11b], according to the formula $\alpha_B = e\hbar^2/4\pi^2\mu e^2$, where ϵ is the static dielectric constant, \hbar is the Planck constant, μ is the reduced mass of an electron hole pair, $1/\mu = 1/m_e + 1/m_h$, m_e and m_h are the effective mass of an electron and hole, respectively, and e is the electronic charge. The calculated α_B of bulk In_2O_3 is about 2.14 nm.
- [20] K. Vanheusden, W. L. Warren, C. H. Seager, D. R. Tallant, J. A. Voigt, B. E. Gnade, *J. Appl. Phys.* **1996**, 79, 7983.

Sub-Nanometer Noble-Metal Particle Host Synthesis in Porous Silica Monoliths

By Lyudmila M. Bronstein,* Sebastian Polarz, Bernd Smarsly, and Markus Antonietti

The functionalization of mesoporous silica with inorganic compounds provides a vast variety of materials that receive significant attention nowadays. Two main applications are catalysis^[1–5] and optical materials.^[5–7] For the catalytic applications, the most essential characteristics are an interpenetrating pore structure of mesoporous oxides and the smallest-pos-

sible catalytic particles located within the pores, which can provide a huge surface area and superior catalytic properties in hydrogenation, oxidation, Heck reaction, and others. For optical materials, particle size, particle size distribution, and regular particle location are crucial, so the ordered mesoporous oxide can also be a perfect host for inclusion of optically interesting particles in 3D structures.

In this communication a very effective method for synthesis of tiny (sub-nanometer) noble-metal particles evenly distributed in the mesoporous monolithic host is presented.

Six general methods of inorganic functionalization of mesoporous silica can be considered. One approach is the addition of inorganic compounds (metal salts or alkoxides) to the sol-gel mixture; in this way a modifying metal is introduced in the silica body, but not necessarily placed in the silica pores.^[8,9] Another method is surfactant replacement by transition metal cations.^[10,11] In this case, metal cations line the interior pore surface but the choice of metal compounds is rather limited. The third method is given by the simple impregnation of calcined silica with solutions of the desired salt followed by reduction or thermal decomposition of metal compounds.^[4,12] This way normally provides the active incorporation of metal compounds inside the pores, though and often restricted by the pore size, and particle growth is not controlled (particle size distribution is broad and particles are located statistically). Chemical vapor deposition instead of impregnation^[4] seemed to be a better way to control nanoparticle growth and particle spreading, but should be restricted only to thin silica films or silica particles (not to monolithic samples) to prevent uneven distribution within the material. The fourth method is the templating of mesoporous silica over metal-containing templates.^[13–15] When metal nanoparticles are located in the block copolymer micelle cores^[13] or in microgels,^[14] and these polymeric structures are used as templates for silica casting, both pore size and metal particle growth control can be approached in such a procedure. The fifth route to inorganically functionalized particles is organic functionalization of silica walls followed by interaction with metal compounds. This avenue has been widely explored and can be realized either through co-condensation of trimethylorthosilicate or tetraethylorthosilicate with organically modified silanes^[5,16] followed by inorganic modification^[17] or by stepwise organometallic modification of silica walls after calcination.^[18–20] The final method, which deserves special attention because of its simplicity, is the direct inorganic modification of silica via interaction with its silanol groups.^[2,5,21] However, inorganic modification after calcination usually leads to a rather limited degree of modification due to the rarity of accessible silanol groups.

Despite the wide variety of methods, to our knowledge, the synthesis of small, sub-nanometer metal particles within the pore system has been reported only once.^[4] Although this step might be regarded as an important accomplishment in tailoring efficient catalytic systems, to increase the metal surface area and to obtain small particles, chemical modification of the pore surface was still necessary.^[4]

[*] Dr. L. M. Bronstein
Department of Chemistry, Indiana University
Bloomington, IN 47405 (USA)
E-mail: lybronst@indiana.edu
S. Polarz, B. Smarsly, Prof. M. Antonietti
Max Planck Institute of Colloids and Interfaces Golm,
D-14424 Potsdam (Germany)

In the present communication for the first time we report a robust and easy way for the inorganic modification of silica monoliths, which are promising, technologically suitable catalysts for tubular reactors. Monolith formation has been reported by a number of authors.^[22–25] When an ordered mesoporous monolith is obtained, very careful extraction and drying are necessary to prevent cracking of the monolith material. The advantages of non-calcined monoliths are: i) preservation of silanol groups on the pore surface, which provide its high functionality and reactivity, and ii) prevailing of inner surface over outer one; the latter is very high for particulate silica powders and can negatively influence the metal particle formation (particles have broad particle size distribution) and the selectivity of reactions. As found recently,^[26] silanol groups are able to interact actively with Pd and Pt anions, presumably through hydrogen bond formation. In this communication we describe the interaction of PdCl_4^{2-} , PtCl_4^{2-} , and PtCl_6^{2-} with silica monoliths templated with a block copolymer (polystyrene-*block*-poly(ethylene oxide), SE1010)^[22] and metal nanoparticle formation from those precursors governed by high functionality of the non-calcined silica host.

The silica monoliths were prepared as described elsewhere.^[22] To demonstrate that the inner structure of the supercritically extracted monolith (using supercritical CO_2)^[25] is similar to calcined silica cast over the same template, transmission electron microscopy (TEM) was employed. The images show that they are nearly identical, though for the extracted species, the pore walls seem to be thicker, corresponding to the lower degree of condensation. Thermogravimetric analysis (TGA, 20–800 °C in O_2) shows that at least 90–95 % of the template is removed by extraction. Metal-salt containing monoliths were prepared by immersion of wet monolith pieces in the aqueous solutions of corresponding potassium salt (10^{-2} mol/L) for 3 days. For the Pd species (PdCl_4^{2-}), the metal salt uptake in the monolith body was fast and observable by the naked eye, since the monolith turned dark brown within several hours. For the Pt salts, the change was slower and less pronounced, whereby the planar PtCl_4^{2-} was still faster than the octahedral PtCl_6^{2-} . After 72 h, these monoliths were also heavily colored indicating that they act as some type of “ion adsorption resin” specific for transition metal anions by interaction with the silanol groups. Because the filling with metal compound solution occurs in a wet monolith, no capillary forces can be responsible for incorporation of metal compounds. The elemental analysis data for the metal-salt-containing monoliths are presented in Table 1. One can see that the Pd molar content is at least three times greater than the Pt content, while the planar Pt complex binds better than the octahedral. We assume that the major driving force for penetration of this kind of anionic complexes in the monolith is hydrogen bonding with silanol groups, though for Pd, another possible binding mechanism operative at longer contact times (up to 3 days) is substitution of Cl by silanol groups or activated surface water. Binding of the Pd complex obviously occurs much faster and with a higher efficiency.

An image of a Pd-ion-containing monolith is presented in Figure 1. It is seen that the metal loading occurs homogeneously, while no specificity of the surface is found.

Table 1. Characteristics of metal-free and metal-containing silica monoliths.

Monolith	Elemental analysis data on metal		BET surface area [m ² /g]	Approx. pore diameter [a] [nm]
	[wt.-%]	[mol.-%]		
metal-free	–	–	745	3.8
K_2PdCl_4	0.91	8.58×10^{-5}	705	3.8
+ H_2 reduction			439	3.7
+ NaBH_4 reduction			396	6.0
K_2PtCl_4	0.51	2.61×10^{-5}	698	3.6
+ H_2 reduction			626	3.9
+ NaBH_4 reduction			421	9.0
K_2PtCl_6	0.39	2.00×10^{-5}	709	3.6
+ H_2 reduction			665	3.8
+ NaBH_4 reduction			413	6.0

[a] From Barrett–Joyner–Halenda (BJH) desorption curve, pure silica is assumed.



Fig. 1. Pd-ion-containing silica monolith in water. The monolith is evenly colored by incorporation of Pd salt (metal-free monolith is almost colorless) for 3 days.

After a 3 day incubation time, the monoliths were washed in water for 24 h. Conductivity measurements on this washing solution show that the Pd precursor is not released from the monolith, while PtCl_4^{2-} is released very slowly and PtCl_6^{2-} is released relatively fast. After washing, the metal-salt-containing monoliths were reduced with hydrogen or with NaBH_4 . The NaBH_4 reduction occurs very vigorously, and the monolith turns dark brown immediately after immersion in the NaBH_4 solution. The hydrogen reduction proceeds slowly and requires elevated temperatures (50 °C) for the Pt compounds. Wet metal-containing samples were examined by small-angle X-ray scattering (SAXS), while for TEM, Brunauer–Emmett–Teller (BET) absorption, and wide-angle X-ray scattering (WAXS) measurements, samples (including metal-free monolith) were dried for 24 h at 60 °C in vacuum.

The SAXS patterns of the metal-containing silica monoliths are nearly identical to the metal-free silica monolith, though the mean value of scattering intensity is much higher than that of pure silica. This demonstrates that the metal centers are located regularly along or in the pore walls of the monolith, which just increases scattering contrast (no new scattering pattern appears). The TEM image of the Pd-containing silica monolith (Fig. 2) is similar to that of metal-free monolith

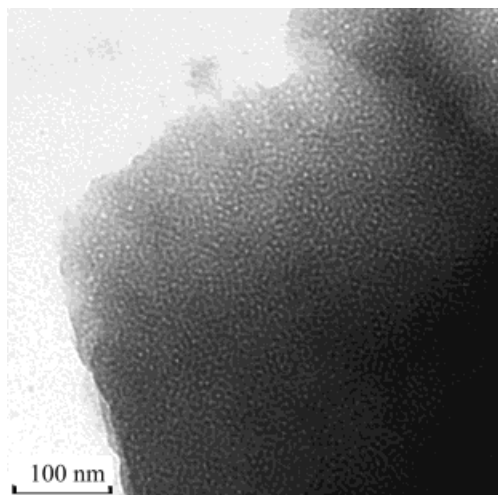


Fig. 2. TEM image of Pd-nanoparticle-containing silica monolith.

(forms interpenetrating pore system) but again the pore walls are much better contrasted. No metal particles can be detected, which means that they are smaller than the resolution of our electron microscope (about 1 nm). Also, WAXS analysis shows no presence of crystallites with a distinguishable size (larger than 1 nm). Analogous results were obtained for Pt nanoparticles prepared with both reducing agents. Thus, TEM, WAXS, and SAXS demonstrate the formation of tiny particles evenly distributed at or in the monolith pore walls. Similar data were reported previously^[4] when a Pd compound was incorporated by chemical vapor deposition and strong interaction with the pore wall was expected. The absence of any obvious dependence of the metal particle size on the type of reducing agent shows that the particle size is not determined by the rate of nucleation but rather is restricted by the strong interaction with the pore walls.

The comparison of the N_2 adsorption isotherms of both the unloaded and the metal-containing monoliths gives a good indication of where the metal particles are located. The unloaded silica as well as silica containing metal complexes possess the typical isotherm shapes for materials containing both meso- and micropores, which is characteristic of silica templated from non-ionic surfactants or block copolymers.^[22,27] Unlike organic modification of mesoporous materials,^[3,28,29] incorporation of the Pd and Pt complexes does not change the pore diameter of the monolith (though their surface area, Table 1, slightly decreases) indicating that ions tightly line the surface of the pores similar to the case described elsewhere.^[10] The practically quantitative preservation of the micropores also shows that the metal complexes are not located in the micropores or block their entries.

After reduction, this situation is changed. The BET curves are dominated by the mesopores, while nitrogen adsorption in micropores is practically absent. This is paralleled by a decrease of the surface area from about $700 \text{ m}^2/\text{g}$ to about $400 \text{ m}^2/\text{g}$, independent of the reduction technique (Table 1). We can only assume that the Pt and Pd particles are nucleated at the micropore entries, which is energetically favorable for

both curvature and functionality density reasons. The noble metal clusters then grow until they block the entries to the micropore system. This is more pronounced for Pd particles because the Pd content in monolith is significantly higher than that of Pt. Since the micropores have a diameter of about $0.3\text{--}0.7 \text{ nm}$,^[27] this mechanism would give an additional reason for the observed very effective restriction to the ultra-small sizes of the noble metal clusters, which is rather unexpected and usually very hard to obtain. It is also underlined that a change in the reducing agent for Pd and Pt compounds does not change the noble metal particle size. It is well known from similar experiments^[30,31] that hydrogen is a much slower reducing agent and usually leads to much bigger noble metal particles. Obviously, the restriction of the particles towards the micropore entries is a very efficient confinement effect, which makes kinetic effects of secondary importance.

A molecular picture of the process can be used to illustrate the complete process. Considering PtCl_4^{2-} and PdCl_4^{2-} as planar discs with a radius of 0.41 nm , a surface area of about 0.53 nm^2 , and a thickness of approximately 0.2 nm , and assuming a surface density of silanol groups of 5 per nm^2 ,^[28] then the limit of incorporation is of the order of one metal ion per square nanometer of silica (thus allowing multiple hydrogen bonding of the complex). A monolith with a mesopore area of about $400 \text{ m}^2/\text{g}$ then contains a maximum of 4×10^{20} Pd ions/g. Based on the van der Waals radius of palladium (0.163 nm) and assuming a particle diameter of about 0.7 nm , it is calculated that clusters with the “magic number” of 13 atoms (octahedron constructed from one layer of spheres around the central sphere) might be generated to block the pores, i.e., about 3×10^{19} nanoparticles/g can be generated.

Experimentally, the described example of Pd-silica (0.9 wt.-% Pd ; 12 g/cm^3 is the density of bulk Pd) contains about 4×10^{18} Pd nanoparticles/g or 5×10^{19} Pd ions/g, which is still well below the limiting value calculated above: the silica surface is therefore far from being saturated with the complex.

A second aspect for discussion is that reduction with NaBH_4 leads to a strong increase of the apparent pore size that is not paralleled by the corresponding drop of the absolute surface area. In addition, both TEM and SAXS indicate that the architecture and sizes of the mesopore system remain unaltered throughout the borohydride reduction. This effect is due to the fact that we have changed the adsorption power by doping the silica surface with the side product of the reduction, the borates, i.e., we have changed the surface structure and chemistry of the glass from a pure quartz glass to a borate glass. This has to be considered for catalytic applications, and hydrogen reduction is certainly preferred when a clean model system is demanded.

To show the superiority of the synthesis within fresh, activated monoliths, metal-compound incorporation, and metal-particle formation was studied in a regular calcined silica cast over SE10/10, which forms the same pore structure. The major difference between the fresh monolith and the calcined silica

is the amount of silanol groups in and on the pore walls. The simple calculation of silanol group density, with the assumption that 47%^[28] of surface Si atoms contain a silanol group, gives a value of about five groups per square nanometer. Calcination at 500 °C for 16 h completes condensation among the adjacent silanol groups. It was found that the amount of silanol groups in calcined silica is equal or less than 30% of the initial amount.^[28]

Incorporation of K₂PdCl₄ and K₂PtCl₄ in calcined silica was carried out by 72 h impregnation of their corresponding aqueous dispersions, followed by isolation, washing, and drying. This resulted in materials containing 0.40 wt.-% Pd or 0.77 wt.-% Pt. By WAXS, a mean particle size for the Pd sample prepared by hydrogen reduction of 5 nm is found. The TEM micrograph (Fig. 3) shows that the Pd particles have an irregular size and shape and are statistically distributed in the material. Thus, the lack of active functionality is clearly reflected in the altered hybrid morphology.

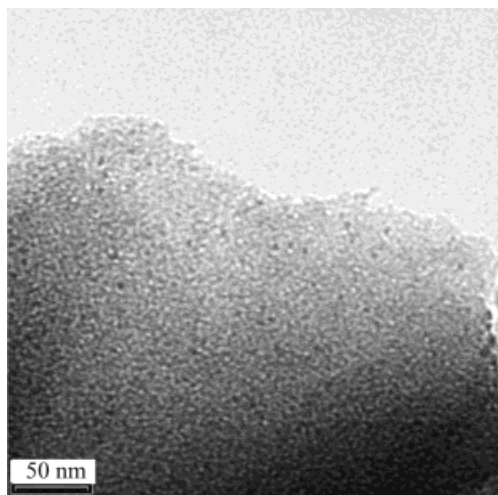


Fig. 3. TEM image of Pd-containing previously calcined silica.

On the other hand, when instead of silica monolith, particulate silica is used where template removal is carried out by extraction and silica silanol groups are mainly preserved, metal particle formation is also largely uncontrolled: along with tiny sub-nanometer particles, large, broadly distributed particles with diameter up to 4 nm are formed due to huge outer surface and particle nucleation at the outer pore entries. This fact emphasizes the crucial role of monolith in the controlled metal nanoparticle formation.

To conclude, we developed a robust method for synthesis of sub-nanometer noble-metal particles regularly located along the pore walls by using the natural functionality of freshly prepared silica monoliths. Loading with appropriate metal complexes and metal particle formation does not change the mesopore structure, while the micropores can be blocked through reduction. The metal particle size is not influenced by the type of reducing agent, which is very unusual and speaks for a very effective mechanism of size restriction, presumably via a template mechanism of the entries of the micropore sys-

tem where noble metal particles are forced to nucleate, but restricted from growth beyond their cavity. The formation and stabilization of such tiny particles (about 0.7 nm in diameter) in highly porous material opens exciting prospects for catalytic applications.

Received: January 22, 2001

Final version: April 4, 2001

- [1] J. Y. Ying, C. P. Meher, M. S. Wong, *Angew. Chem. Int. Ed.* **1999**, *38*, 56.
- [2] M. S. Morey, J. D. Bryan, S. Schartz, G. D. Stucky, *Chem. Mater.* **2000**, *12*, 3435.
- [3] J. Liu, X. Feng, G. E. Fryxell, L.-Q. Wang, A. Y. Kim, M. Gong, *Adv. Mater.* **1998**, *10*, 161.
- [4] C. P. Mehnert, D. W. Weaver, J. Y. Ying, *J. Am. Chem. Soc.* **1998**, *120*, 12 289.
- [5] K. Moller, T. Bein, *Chem. Mater.* **1998**, *10*, 2950.
- [6] H. Shi, L. Zhang, W. Cai, *J. Appl. Phys.* **2000**, *87*, 1572.
- [7] K. W. Powers, L. L. Hench, *Ceram. Trans.* **2000**, *101*, 253.
- [8] T. Sun, J. Y. Ying, *Nature* **1997**, *389*, 704.
- [9] G. Fryxell, J. Liu, *Surf. Sci. Ser.* **2000**, *90*, 665.
- [10] M. Yonemitsu, Y. Tanaka, M. Iwamoto, *Chem. Mater.* **1997**, *9*, 2679.
- [11] A. R. Badiei, L. Bonneviot, *Inorg. Chem.* **1998**, *37*, 4142.
- [12] M. H. Huang, A. Choudrey, P. Yang, *Chem. Commun.* **2000**, 1063.
- [13] L. Bronstein, E. Krämer, B. Berton, C. Burger, S. Förster, M. Antonietti, *Chem. Mater.* **1999**, *11*, 1402.
- [14] N. T. Whilton, B. Berton, L. Bronstein, H.-P. Hentze, M. Antonietti, *Adv. Mater.* **1999**, *11*, 1014.
- [15] A. A. Eliseev, A. V. Lukashin, A. A. Vertegel, L. I. Heifets, A. I. Zhironov, Y. D. Tretyakov, *Mat. Res. Innovat.* **2000**, *3*, 308.
- [16] D. S. Shephard, W. Zhou, T. Maschmeyer, J. M. Matters, C. L. Roper, S. Parsons, B. F. G. Johnson, M. J. Duer, *Angew. Chem. Int. Ed.* **1998**, *37*, 2719.
- [17] O. Kröcher, R. A. Köppel, M. Fröba, A. Baiker, *J. Catal.* **1998**, *178*, 284.
- [18] W.-H. Zhang, J.-L. Shi, L.-Z. Wang, D.-S. Yan, *Chem. Mater.* **2000**, *12*, 1408.
- [19] B. Lebeau, C. E. Fowler, S. Mann, C. Farcet, B. Charleux, C. Sanchez, *J. Mater. Chem.* **2000**, *10*, 2105.
- [20] L. Zhang, T. Sun, J. Y. Ying, *Chem. Commun.* **1999**, 1103.
- [21] S. Dai, M. C. Burleigh, Y. Shin, C. C. Morrow, C. E. Barnes, Z. Xue, *Angew. Chem. Int. Ed.* **1999**, *38*, 1235.
- [22] C. G. Göltner, S. Henke, M. C. Weissenberger, M. Antonietti, *Angew. Chem. Int. Ed.* **1998**, *37*, 613.
- [23] P. Feng, X. Bu, G. D. Stucky, D. J. Pine, *J. Am. Chem. Soc.* **2000**, *122*, 994.
- [24] N. A. Melosh, P. Davidson, B. F. Chmelka, *J. Am. Chem. Soc.* **2000**, *122*, 823.
- [25] N. Hüsing, U. Schubert, K. Misof, P. Fratzl, *Chem. Mater.* **1998**, *10*, 3024.
- [26] D. I. Svergun, M. B. Kozin, P. V. Konarev, E. V. Shtykova, V. V. Volkov, D. M. Chernyshov, P. M. Valetsky, L. M. Bronstein, *Chem. Mater.* **2000**, *12*, 3552.
- [27] C. Göltner, B. Smarsly, B. Berton, M. Antonietti, *Chem. Mater.* **2001**, in press.
- [28] L. Mercier, T. Pinnavaia, *Env. Sci. Technol.* **1998**, *32*, 2749.
- [29] J. Liu, Y. Shin, Z. Nie, J. H. Chang, L.-Q. Wang, G. E. Fryxell, W. D. Samuels, G. J. Exarhos, *J. Phys. Chem.* **2000**, *104*, 8328.
- [30] M. Antonietti, E. Wenz, L. Bronstein, M. Seregina, *Adv. Mater.* **1995**, *7*, 1000.
- [31] S. Klingelhöfer, W. Heitz, A. Greiner, S. Oestreich, S. Förster, M. Antonietti, *J. Am. Chem. Soc.* **1997**, *119*, 10116.